Environmental Electroactive consortia as reusable biosensing element for freshwater toxicity monitoring

V. Agostino, G. Massaglia, M. Gerosa, A. Sacco, G. Saracco, V. Margaria, M. Quaglio

PII: S1871-6784(18)30077-3

DOI: https://doi.org/10.1016/j.nbt.2019.09.005

Reference: NBT 1204

To appear in: *New BIOTECHNOLOGY*

Accepted Date: 24 September 2019

Please cite this article as: Agostino V, Massaglia G, Gerosa M, Sacco A, Saracco G, Margaria V, Quaglio M, Environmental Electroactive consortia as reusable biosensing element for freshwater toxicity monitoring, *New BIOTECHNOLOGY* (2019), doi: https://doi.org/10.1016/j.nbt.2019.09.005

Environmental Electroactive consortia as reusable biosensing element for freshwater toxicity monitoring

V. Agostino[a,b], G. Massaglia[a,b], M. Gerosa[a,b], A. Sacco[a], G. Saracco[a], V. Margaria[a,*] and M. Quaglio[a]

[a] Center For Sustainable Future Technologies @Polito, Istituto Italiano Di Tecnologia, Via Livorno 60, 10144 Torino, Italy

[b] Department of Applied Science and Technology, Politecnico di Torino, 10129 Torino, Corso Duca Degli Abruzzi 24, 10129 Torino, Italy

*corresponding author: **valentina.margaria@iit.it**

Graphical abstract

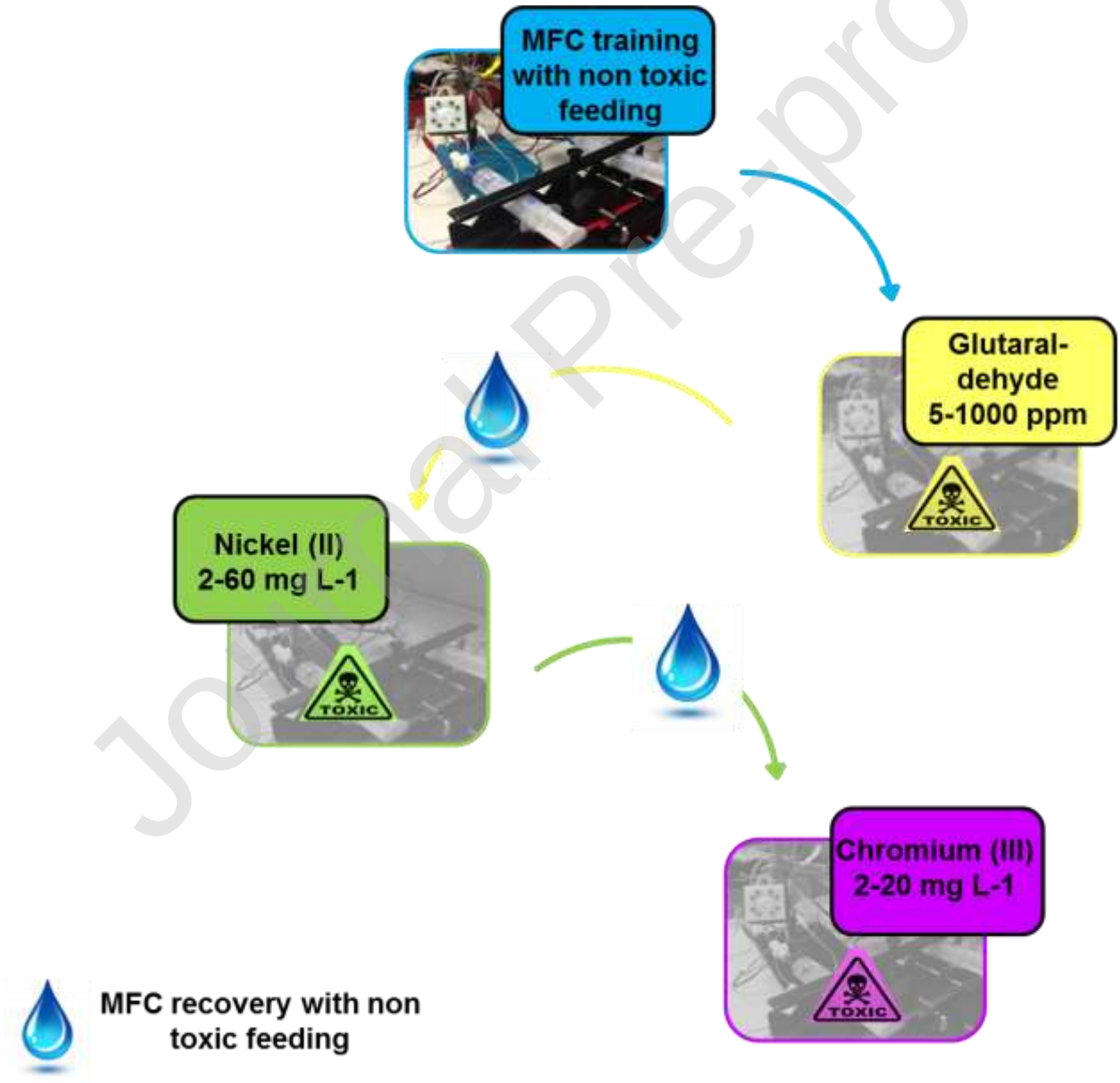

Highlights

- Electroactive river sediment consortium as biosensing element for water monitoring
- Sensitivity towards different toxicants: glutaraldehyde, nickel(II) and chromium(III)
- Reusability of the Microbial Fuel Cell based biosensor
- Novel algorithm for efficient and energy saving data analysis

Abstract

The development of tools to monitor water quality is mandatory in a scenario where clean water resources are decreasing. Here, the biosensing capability of an electroactive river sediment consortium was tested towards three model contaminants (glutaraldehyde, nickel(II) and chromium(III)). The proposed biosensor is a small membrane-less single chamber Microbial Fuel Cell (MFC), fabricated by 3D printing. Its semi-continuous mode of operation resulted in long-term current profile stability and reproducibility. A linear trend of response was obtained for glutaraldehyde in a concentration range of 5-1000 ppm. After the recovery of the electroactive consortium activity, the MFC-based biosensors were shown to be sensitive towards Ni(II) and Cr(III), at concentrations above 2 mg L^{-1}. To effectively analyze biosensor response, a novel algorithm was proposed, offering advantages for the realization of energy-saving protocols for MFC-biosensor data transmission. Implementation of the device and method, from laboratory test to real environment, can offer a low cost *in situ* system for detection of water contaminants.

Keywords: electroactive river sediment consortium, reusable biosensor, Microbial Fuel Cell (MFC), water toxicity, glutaraldehyde, heavy metals

Introduction

Water scarcity and poor water quality have a negative impact on food security, livelihood choices and educational opportunities across the world. For these reasons guaranteed access to clean water is one of the 17 Sustainable Development Goals defined by the United Nations during the Sustainable Development Summit in 2015 [1]. Water scarcity affects more than 40% of the world's population and at least 1.8 billion people globally use a source of drinking water that is contaminated. More than 80% of wastewater resulting from human activities is discharged into rivers or seas without any pollutant removal, thus reducing the water quality [2]. One of the six targets related to the clean water challenge is to improve water quality by 2030 by reducing pollution, eliminating dumping and minimizing the release of hazardous chemicals and materials [2]. At the same time, the implementation of water management and *in situ* water quality monitoring systems is fundamental to controlling and providing access to clean water.

To ensure effective monitoring and treatment programs, complementary methods are required [3]:

(i) As a first step, an *in situ*, low cost, non-specific early warning system which can be operated online.

(ii) As a second step, accurate detection and quantification of specific pollutants through conventional analytical methods, which are more time consuming and expensive and require trained operators.

Microbial Fuel Cells (MFCs) represent a promising biotechnological approach to direct conversion of the chemical energy stored in organic matter into electricity, through reactions catalyzed by electroactive microorganisms. The technology was developed initially for wastewater treatment with simultaneous energy recovery [4–7]. In the last decade, increasing attention has been paid to the potential use of MFCs as water quality monitoring systems. Notably, MFC-based biosensors have been proposed for the detection of toxic compounds [8] and the measurement of biochemical oxygen demand (BOD) of water samples [9].

Biosensors are based on a biological sensing element combined with a physical transducer which converts the biological signal into a detectable one, such as electrical current [10]. In MFC-based biosensors, microbial metabolism is the sole driving force for conversion of the chemical energy into electrical energy and thus the sensing and signal transduction steps are integrated in a single element, without the need of a transducer and an external power source. Moreover, MFC-based biosensors are rapid response early detectors, which are simple in operation and can be highly cost effective, as they can be constructed using low cost carbon-based materials [11, 12]. Unlike conventional physiochemical methods, which are usually specific towards a single class of molecule, MFC electrical output is affected by many toxicants. Thus, MFC monitoring systems can reveal the presence of a single compound as well as the synergistic effects of complex and unknown pollutants. Thanks to these unique characteristics, MFC-based biosensors can be employed as *in situ* early warning systems for overall water toxicity assessment.

The use of MFC-based biosensors to monitor water quality has recently been reviewed [13]. Most previous studies were concerned with lowering the biosensor detection limits, testing different toxicants and enhancing sensitivity through different device architectures [13]. In particular, little attention has been devoted to the biosensing element. The majority of reports have made use of pure culture exoelectrogens (*Geobacter sulfurreducens* and *Shewanella oneidensis*) [14, 15, 18, 19] or mixed consortia taken from long-term operated MFCs [16, 17, 20-23]. However, in order to provide a long lasting biosensing element for the development of an *in situ* water alarm detector system, the inoculum source is crucial. Mixed community consortia coming directly from the environment are likely to be more resilient and require less maintenance then a pure culture. Moreover, microbial activity and MFC performance are significantly affected by conventional MFC operational parameters such as pH, temperature, external load and substrate concentration [24–27]. Most of the work simulating toxicant events in order to test the biosensing ability of MFCs was usually performed under controlled laboratory conditions, such as fixed temperature, without taking into consideration the environmental variation of this parameter [8, 14–17].

Focusing on the development of a long-term, reusable alarm detector for *in situ* river water quality monitoring, the aim of this study was to investigate the biosensing capability of an electroactive consortium derived from a river sediment sample. The bioanode sensitivity was tested at laboratory scale towards three model contaminants in small membrane-less single-chamber MFCs, under non-controlled room temperature (RT) conditions, while ensuring a fixed organic concentration load and a constant pH of 7. Biosensor performance was evaluated in terms of inhibition ratio,

linearity of the response and recovery. Finally, a new algorithm to implement data transmission and analysis was proposed.

Materials and Methods

In order to aid understanding of the experimental work flow, an overview of all the different MFCs working phases is presented in **Figure** 1.

Inoculum preparation

A river sediment sample (from Valle D'Aosta, Italy) was maintained under anoxic culture conditions before inoculation into the MFCs, using acetate as organic source for the microbial enrichment. The enrichment medium was selected based on [28], where two different media were tested for the enrichment phase. The difference between the two media consisted in the presence or absence of Iron (III) Citrate as electron acceptor. Enrichment without electron acceptor resulted in better performing MFCs [28]. Based on these results, the enrichment medium consisted of NH_4Cl 1.50 g L^{-1}; NaH_2PO_4 2.45 g L^{-1}; Na_2HPO_4 4.28 g L^{-1}; KCl 0.10 g L^{-1}; Na-acetate 2.50 g L^{-1}; Wolfe's Vitamin solution 10.00 mL L^{-1} (MD-VS**,** ATCC, Virginia, USA) and Wolfe's trace mineral solution 10.00 mL L^{-1} (MD-TMS™, ATCC, Virginia, USA).

The microbial cultures were subjected to 2 subculturing steps for a total growth of 15 d, at RT and with gentle orbital shaking (150 rpm). The subculturing step consisted in the exchange of 90% of the liquid culture with fresh medium.

MFC design

The membrane-less single chamber MFCs in an open-air cathode configuration were fabricated by 3D-printing (OBJET 30, Stratasys), using a polymeric UV-curable polymer (Figure S1) [29]. The anode and cathode electrodes were made of commercial Carbon Felt (CF) (Soft felt SIGRATHERM GFA 5, SGL Carbon, Germany); the area of both was 9 cm^2 and the total inner chamber volume was 12.5 mL. Both liquid inlet and outlet were on the same plane in the z-direction (where the z-axis describes the thickness of the chamber), but nonsymmetrical in the x-y plane (Figure S1C). Stainless steel wires were threaded along the carbon felt for the electrical contacts. The open-air cathode was made from CF modified following the method adopted in the literature [30]. In particular, a layer of platinum was deposited on CF as catalyst and, on the opposite side of CF, polytetrafluoroethylene (PTFE) was deposited as an oxygen diffusion layer.

MFC acclimation and start-up

Laboratory experiments were conducted under non-controlled RT conditions. The temperature was monitored with an EBI 300 Temperature Data Logger (Bartscher GmbH, Germany) and was in the range 20±4°C. Four MFCs were inoculated with the microbial culture derived from the second step of enrichment of the river-sediment (10% v/v). Anodic biofilm acclimation was performed for 10 d using a low external resistance (47 Ω), resulting in a positive anode potential polarization. The voltage of MFCs was acquired every 5 min by a digital multimeter (34972A, Keysight Technologies, CA, USA). The resultant current (I) was calculated using Ohm's law (I= V /Rext) and the current density (j) was obtained after normalizing the current for the electrode surface area. During the acclimation period, MFCs were maintained in batch condition for 5 d to allow biofilm formation and then operated in continuous mode using a

hydraulic retention time (HRT) of 5 d in order to avoid microbial biomass washout from the devices and to provide continuous feeding for the biofilm on the anode. The electrolyte was pumped inside the MFCs using multiple channel syringe pumps (NE1600, New Era Instrument, USA). After acclimation, two different external resistances (47Ω and 1kΩ) were tested. The electrolyte had the same composition of the enrichment medium, but with a lower concentration of Na acetate ($1gL^{-1}$).

Biosensing experiment

Before starting toxicity tests, MFC feeding was switched to a semi-continuous mode, under 1 kΩ external load. The same medium of acclimation phase was used and was pumped inside the device for 4 h per d with an HRT of 1 h. After several stable and repeatable non-toxic feeding cycles, all toxicity tests were carried out in duplicate (using the two MFCs that operated at 1kohm after the start-up period), under non-controlled temperature conditions (20±4 ^{o}C).The MFCs were fed with different concentrations of glutaraldehyde (5-1000 ppm) dissolved in the basal medium. Each toxicant event was followed by recovery cycles (from 1 to 4 cycles) with non-toxic medium, in order to reobtain a stable baseline current before increasing the amount of glutaraldehyde into the influent or changing toxicant type. Ni^{2+} toxic events were performed at concentrations of 2 mg L^{-1}, 20 mg L^{-1} and 60 mg L^{-1}, achieved by dissolving $Ni(NO_3)_2$ hexahydrate into the basal medium. Cr^{3+} toxicant events were performed at concentrations of 2 mg L^{-1} and 20 mg L^{-1}, achieved by dissolving $Cr(NO_3)_3$ nonahydrate in MFC influent.

To evaluate performance of the MFCs, the inhibition ratio (I) induced by the different toxicants was calculated according to [8] by the following equations:

a. Inhibition ratio at 4 h: I_{4hs} (%) = 100 x (j_{nor} - j_{tox})/j_{nor}
b. Inhibition ratio based on total coulombic yield: I_C (%) = 100 x (C_{nor} - C_{tox})/C_{nor}

In Equation **a.** $\mathbf{j_{nor}}$ is the current density generated by the MFC after 4 h of non-toxic feeding and $\mathbf{j_{tox}}$ is the current density output after 4 h of toxic influents.

In Equation **b.** $\mathbf{C_{nor}}$ is the total coulombic yield under non-toxic conditions, while $\mathbf{C_{tox}}$ is the total coulombic yield obtained in toxic conditions. The total coulombic yield represents the sum of charges produced in one fed-batch cycle (24 h).

Biosensing response data analysis

The first derivative of the current density as a function of time was calculated for non-toxic cycles (at least 2 before the evaluation of a new toxicant) to identify maxima and minima used to pick out the Critical Time Points (ctps) of the function. Three ctps were identified.

The exact time/minute related to a ctp is the result of the average of 2 non-toxic cycles:

c. Time /minute $ctp_X = (ctp_{Xcycle1}+ctp_{Xcycle2})/2$

The current density value assigned to each ctp is the average of 5 measurements centered around the ctp observed:

d. Current density value for ctp$_X$ = j_{ctpx} = $\frac{\sum_{n=-2}^{2} j_{y+tn}}{5}$

In Equation **d, j_y** is the current density at time point **y**/minute while ***t*** is the sampling rate (in this case 5 min).

The inhibition value for each ctp was calculated as:

e. Inhibition value at a specific ctp$_X$: I_{ctpx} (%) = 100 x ($j_{ctpxnor}$ - $j_{ctpxtox}$)/$j_{ctpxnor}$

Where j_{ctpnor} is the current density value associated with the specific ctp (based on eq. d) for non-toxic feeding and j_{ctptox} is the current density value associated with the specific ctp for toxic influents.

The process used to analyze the data is described graphically in Supplementary Figure S2.

Results and Discussion

Biofilm start-up and current production under different external loads

Four MFCs were inoculated with enriched river-sediment cultures (10% v/v) and the current production under 47 Ω was monitored. This low external resistance acclimation method has been demonstrated previously to improve start-up and current generation of MFCs [28; 31–33]. MFCs, acclimated at RT (20±4°C), showed a start–up time of 5 d, reaching a current density of 450 mA m^{-2} after 10 d (data not shown). The effect of external resistance was investigated in terms of current stability under non-toxic conditions, in order to establish the best working conditions and to obtain a stable baseline current during non-controlled temperature operation. After bioanode acclimation, two external loads were tested, 47Ω and 1kΩ. The laboratory temperature was monitored, while pH and the organic substrate were maintained at a constant level.

Figure 2 shows the different baseline currents obtained and the temperature variation profile. Under low external resistor, the MFCs exhibited a high sensitivity to emperature fluctuation with a current density average in 7 d of 493± 125 mA m^{-2} (MFC_c) and 615± 118 mA m^{-2} (MFC_d) , and coefficient of variation (CV) of 25.4% (MFC_c) and 19%(MFC_d), while those under 1 kΩ resistor generated a more stable current density with a lower CV value of 4% for MFC _a and 9 %for MFC_b (current density average in 7 d was 409 ±18 mA $m^{-2}$and 415± 39 mA m^{-2}). Based on these results, 1kΩ external load was chosen as control mechanism for the MFC-based biosensor toxicity tests. As far as we are aware, only one group [24] has studied the effect of different external loads for MFC-based biosensor application. They showed that high external resistance (1 kΩ) resulted in a smaller current change during the toxicant event compared to a lower resistance of 100 Ω, but a faster recovery time of the biosensor. In that work the toxicity tests were performed under a controlled temperature of 30° C.

Non-toxic operation of MFC-based biosensors.

The sensors were operated indoors with an RT variation in the range of 16°C to 24°C. However, in real environments, larger temperature variations can be expected, depending on the climatic area of the river to monitor. As observed in [45], during MFC field tests performed in sea water the temperature fluctuation during day/night cycle had visible effects on current production. In contrast, no appreciable differences between summertime and wintertime operations was evidenced concerning MCF performance, despite a 10°C temperature variation. This effect is probably

due to the ability of the microorganisms to adapt their metabolism progressively to the gradual temperature decrease between summer and winter. The results observed during a day/night cycle can be associated with a rapid temperature change which did not allow metabolic adjustment or adaptation [45].

Based on these results, before starting the toxicity tests, the MFC feeding modality was switched to a semi-continuous mode (see Methods). In this operation mode, biosensor feeding always starts at the same time during the day, and can mitigate the effect of temperature fluctuations during the day/night cycle, reducing the current output variability due to environmental parameters. Moreover, *in situ* application for effective water quality monitoring requires several sensors to be organized in a network, where every MFC represents a node of the sensor network [46]. In this view, the aim of the semi-continuous operation mode is to enhance power management within the network. By operating each device at a defined time interval (e.g. 4 h per day), the power management system required to monitor the sensor network was not forced to work throughout the day, thus extending its operating life [34]. The sensors were trained with several (5) cycles carried out with non-toxic influent at a fixed concentration of acetate (1 g L^{-1}).

As shown in **Figure 3**, the different non-toxic cycles had a high level of reproducibility of 99% in terms of current density production after 4 h of feeding and total coulombic yield. The non-toxic current density profile was characterized by a steep increase, corresponding to the feeding entry into the device. This was followed by an inflection point, corresponding to about 2 complete MFC-volume exchanges (2 h). The current continued to increase slowly until it reached its maximum value, after stopping influent feeding. The batch period of the cycle was characterized by a phase of quite constant current generation (~12 hours), followed by a steep current decrease to the background level of 50±5 mA m^{-2}, corresponding to total consumption of the organic substrate.

Toxicity detection: glutaraldehyde, nickel(II) and chromium(III)

An effective on-line monitoring and alert system has to be sensitive to several pollutants. Glutaraldehyde was chosen as a model toxicant, a saturated five-carbon dialdehyde used industrially in several applications, [35,36]. It is characterized by strong biocidal activity due to the alkylation of sulfhydryl, hydroxyl, carboxyl, and amino groups, which alters RNA, DNA and protein synthesis [37]. Sensitivity to the toxic effect of glutaraldehyde was tested at different biocide concentrations, starting from 5 ppm. As shown in **Figure 4**A, even the lowest concentration of glutaraldehyde affected the normal current profile curve observed in non-toxic conditions. At the end of feeding period (4 h), the current decreased in proportion to the increment of biocide concentration. Figure 4B illustrates the current change after 4 h of toxic feeding plotted against the relative concentration of glutaraldehyde. As shown, a linear trend was observed between 5 and 1000 ppm, with R^2 (linear regression coefficient) value of 0.99. With high biocide concentrations (500 and 1000 ppm), the current profile shape was altered and only a peak followed by a constant current decrease was observed. To understand the biosensor response, two different elements were analyzed: a single time point inhibition ratio at 4 h (I_{4hs}) and the inhibition ratio based on the total coulombic yield (I_C) (eq. **a** and **b** in Materials and Methods). When glutaraldehyde concentration was equal to, or higher than, 500 ppm the I_{4hs} values agreed with those based on total coulombic yield (I_C) (Figure 4C). In contrast, with low glutaraldehyde concentrations (5 and 50 ppm) the I_{4hs} values and I_C values were discordant: an inhibitory effect was visible only if considering the current density production after 4 h of feeding. A possible explanation lies in the metabolism of

glutaraldehyde which is sufficiently rapid under both aerobic and anaerobic conditions ($t_{1/2}$ 7.7 h)to allow a rapid recovery of microbial activity if the biocide concentration is very low [36]. Increased concentrations of glutaraldehyde, equal to or higher than 500 ppm, strongly affected the metabolic activity of the bioanode and the current production profile.

Untreated or allegedly treated industrial effluents often contain variable amounts of heavy metals, which have the potential to contaminate freshwater resources. Nickel(II) (Ni^{2+}) was chosen as an acute toxic heavy metal, used in the manufacture of many alloys and products. It is released into the environment by power plants, metal factories and waste incinerators. Once recovered from 1000 ppm glutaraldehyde, the sensitivity of the mixed anodic consortium for Ni^{2+} was evaluated (**Figure 5**). Three different concentrations of Ni^{2+} were tested: 2 mg L^{-1}, 20 mg L^{-1} and 60 mg L^{-1}. The biosensors showed tolerance to the lowest concentration of Ni^{2+}, while demonstrating a linear sensitivity towards higher ones (Figure 5B). As shown in Figure 5A, the presence of 20 mg L^{-1} of Ni^{2+} inside the influent led to a decrease in current density production, visible after 4 h of feeding. At 60 mg L^{-1}, the difference in current generation appeared from the start of the feeding cycle. These results are in accord with those in [39] where the response of a wastewater consortium towards Ni^{2+} was tested in a flat membrane-based MFC configuration: 50 mg L^{-1} of Ni^{2+} resulted in a faster MFC voltage drop than 20 mg L^{-1}, while Ni^{2+} 5 mg L^{-1} caused no variation in voltage output. In the present study, high Ni^{2+} concentrations not only generated a reduction in current density production after the end of the feeding step, but also a lower total coulombic yield compared to the non-toxic cycles (Figure 5A), and in consequence the I_{4hs} and I_C values were quite similar (Figure 5C).

The trivalent chromium was selected as heavy metal with a low degree of toxicity, due to its insolubility [40]. Emissions of Cr^{3+} compounds into freshwater may result from leather tanning, chemical manufacturing (e.g. dyes for paints, rubber and plastic products) and metal finishing industries (e.g. chrome plating) [41]. After electroactive consortium recovery from Ni^{2+} 60 mg L^{-1}, Cr^{3+} toxicity tests were performed at concentrations of 2 and 20 mg L^{-1}. The biosensors were tolerant of the lowest concentration, but when it was increased to 20 mg L^{-1} an unusual current density profile was observed. In contrast to the data obtained for Ni^{2+}, a small current density change was observed after 4 h feeding, but with a steep decrease after a few hours of batch condition (Figure 6A). The inhibition ratio based on the total coulombic yield (I_C) was 13.3±1.3 %, while I_{4hs} was only 2.4 ±0.4% (Figure 6B).

This characteristic response underlined a different mechanism of Cr^{3+} bioaccumulation and toxic action towards the anodic consortium, compared to Ni^{2+}. Several distinct types of mechanism are used to import Ni into microbial cells, including specific import through Ni/Co transporter systems (NiCoT family), or non-specific import through the Mg importer CorA or TonB-dependent transporters [38]. In contrast, the mechanisms by which extracellular binding of Cr^{3+} exerts toxicity on microorganisms are poorly characterized. Early studies on the effect of Cr^{3+} towards active sludge suggested that toxicity is related to binding competition with organic substrate for the same active sites of cellular membranes [42, 43]. Our results can be explained in agreement with these reports, developing the following hypothesis. During the feeding part of the cycle, the organic substrate (acetate) was continuously supplied, allowing quite a constant organic load to be maintained, whereas during the batch part the acetate started to be consumed by

the consortium. When the acetate concentration fell, Cr^{3+} could effectively compete with the low level of organic substrate and cross microbial cell membranes, resulting in a steep current decrease.

Reusability of MFC-based biosensors

A critical requirement for on-site water quality monitoring is the ability of the biosensor to restart activity even if damaged by toxic substances. To investigate the reusability of the biosensing element, the same devices were subjected to different pollutants sequentially and each toxic detection test was followed by recovery cycles to reobtain a reproducible and stable baseline current profile. **Figure 7** shows part of the overall toxicity experiment, reporting the non-toxic cycles before starting the biosensing test (sensor training), the toxic cycle with highest pollutant concentrations and their respective recovery cycles. In contrast with other reports on sensitivity of MFC-based biosensors towards toxic aldehydes [14,18], the bioanode employed exhibited the ability to recover activity even after the highest concentration of glutaraldehyde (1000 ppm): 3 recovery cycles were adequate to obtain a stable and reproducible current baseline. This was remarkable since the method used to test responsiveness of the MFCs was characterized by an extended toxic shock. The anodic consortium remained in contact with glutaraldehyde for 24 h during each toxic event, thus allowing the biocide element to diffuse into the biofilm. As shown in Figure 7, the highest concentration of nickel(II) tested (60 mg L^{-1}) required only one recovery cycle to stabilize the baseline current. These results illustrated the strong relationship between biosensor recovery time and toxicity level of the different pollutants. Table 1 shows the comparison of the stable non-toxic feeding cycles before each experiment, in terms of current density values after 4 h feeding and total coulombic yield, and the degree of recovery based on these two parameters.

A new algorithm for data analysis

When dealing with an online and long-term monitoring system, the lifetime of a sensor node depends on the power supply it is equipped with. One way of prolonging the operating life of a sensor network is to implement an efficient communication protocol that can reduce energy consumption for data transmission. Moreover, the classical methods of analyzing MFC-based biosensors (single point analysis or total coulomb yield) appear inadequate to describe the response exhaustively [8]. In order to understand the biosensor response better, while saving energy for data transmission and time for data elaboration, a novel algorithm was proposed. The method is based on the following rules:

(i) Biosensor training with non-toxic influent to obtain reproducible baseline cycles.

(ii) Analysis of the non-toxic current density profile based on the first derivative as a function of time. The maxima and minima of the first derivative function represent the critical time points (ctps) which are selected to analyze the overall response of the sensor. When perturbed by a toxic event, the sensor must be re-trained with non-toxic feeding to relocalize the critical time points correctly.

(iii) After the biosensor training and first derivative analysis, only the data limited to the ctps are transmitted and analyzed to highlight anomalies and toxicants presence in the water. An inhibition value is associated with each ctp based on eq. **e** (Materials and Methods). The sum of the inhibition values represents the Total Toxicity Inhibition (I_{tot}).

As previously discussed, the data demonstrated that I_C values and I_{4hs} sometimes gave discordant information: this is the case for glutaraldehyde at low concentrations and for 20 mg L^{-1} of Cr^{3+} (Figures 4C, 6B). The toxicity of a compound depends on several factors: its mechanism of interaction with the microbial communityand its bioaccumulation and degradation. It is difficult to select the correct parameter to evaluate the toxic effect of a pollutant. Based on the above algorithm, it was possible to identify 3 ctps distributed along the 24 h non-toxic cycle (**Figure 8**). The first (ctp1) represents early-toxicity, the second (ctp2) the mid-term toxicity while the third (ctp3) gives information on late toxicity and the recovery ability of the bioanode within a single cycle. The total toxicity (I_{tot}) corresponds to the sum of the effects observed at each ctp. **Table 2** reports the inhibition values related to the single ctp (I_{ctp}) and the I_{tot} for the pollutants tested. Analyzing the 3 ctps it was possible to speculate about the toxic action of the different compounds. For glutaraldehyde, especially at low concentrations, a fast toxic action was observed, evident at ctps1 and 2, but a low I_{tot} due to the rapid degradation of the dialdehyde and the recovery of biofilm activity. In contrast, for 20 mg L^{-1} of Cr^{3+}, toxicity was not visible at ctp1 and ctp2, however, the overall toxicity I_{tot} was noteworthy, due to the high value of I_{ctp3} e in agreement with Cr^{3+} bioaccumulation mechanisms.

Conclusion

The aim of this work was to explore at laboratory scale the sensing ability of a microbial community from a river-sediment source towards different types of pollutants, for the future development of MFC-based biosensors for quality monitoring of river streams. The semi-continuous operation mode of the MFC-based biosensors allowed high stability of non-toxic current profile to be obtained, even in non-controlled RT conditions and without the use of potentiostatic control of the anodic potential. A linear response towards glutaraldehyde concentrations within the range 5-1000 ppm, was observed. Heavy metals (nickel(II) and chromium(III)) were detected at concentrations higher than 2 mg L^{-1}. All toxicant detection tests were performed towards the same microbial consortium. The river-sediment bioanodes were able to recover their activity after each pollutant concentration tested, with toxic cycle durations of 24 h. These findings highlighted the high versatility and reusability of the electroactive environmental consortia. Nevertheless, contamination events with complex mixtures of pollutants can easily occur. Further investigations with a cocktail of toxicants (e.g. binary and ternary mixtures) are fundamental to assessing the response and recovery ability of the river-sediment bioanodes after a complex toxic shock.

A novel algorithm, identifying critical time points based on the analysis of the first derivative of the current density, was proposed. The results obtained effectively described the overall toxicity of a specific compound and could also provide information about its mode of effect on the anodic consortium, revealing important elements about the different toxicants analyzed. The approach can be employed successfully in an application such as long-term online monitoring, where energy efficiency is a critical concern and therefore an improved communication protocol for data transmission may be necessary to extend the operating life of the sensor node.

The implementation of MFCs as early-warning systems will require further research. For example, COD values vary significantly from river to river and during the whole year, while in the present study a constant COD value of 0.78 g L-1 (= 1 gL-1 acetate) was employed. To overcome this limitation during field application, a solid-state anolyte, able to release constant concentrations of organic substrate over time in the liquid anodic phase, can be employed [44, 45].

Moreover, the concept of the *in situ* colonization method for bioanode development could be explored in order to minimize manual operations and create an electroactive biofilm, avoiding a laboratory acclimation phase and without altering the natural community [45]. Nonetheless, this study provides a proof of concept for the use of river sediment consortia as biosensing elements for toxicity monitoring.

Acknowledgement

The authors thank Simona Pentassuglia and Daniyal Ahmed for their valuable support and the constructive discussions. The research was financially supported by Fondazione Istituto Italiano di Tecnologia.

References

[1] United Nations. Transforming our world: the 2030 Agenda for Sustainable Development. Gen Assem 70 Sess 2015;16301:1–35. doi:10.1007/s13398-014-0173-7.2.

[2] United Nations. Clean Water and Sanitation: Why It Matters. Sustain Dev Goals Briefs 2016:2.

[3] Lagarde F, Jaffrezic-Renault N. Cell-based electrochemical biosensors for water quality assessment. Anal Bioanal Chem 2011;400:947–64. doi:10.1007/s00216-011-4816-7.

[4] Liu H, Liu H, Ramnarayanan R, Ramnarayanan R, Logan BE, Logan BE. Production of electricity during wastewater treatment using a single chamber microbial fuel cell. Environ Sci Technol 2004;38:2281–5. doi:10.1021/es034923g.

[5] Aelterman P, Rabaey K, Clauwaert P, Verstraete W. Microbial fuel cells for wastewater treatment. Water Sci Technol 2006;54:9. doi:10.2166/wst.2006.702.

[6] Rabaey K, Verstraete W. Microbial fuel cells: novel biotechnology for energy generation. Trends Biotechnol 2005;23:291–8. doi:10.1016/j.tibtech.2005.04.008.

[7] Du Z, Li H, Gu T. A state of the art review on microbial fuel cells: A promising technology for wastewater treatment and bioenergy. Biotechnol Adv 2007;25:464–82. doi:10.1016/j.biotechadv.2007.05.004.

[8] Kim M, Sik Hyun M, Gadd GM, Joo Kim H. A novel biomonitoring system using microbial fuel cells. J Environ Monit 2007;9:1323–8. doi:10.1039/b713114c.

[9] Chang IS, Jang JK, Gil GC, Kim M, Kim HJ, Cho BW, et al. Continuous determination of biochemical oxygen demand using microbial fuel cell type biosensor. Biosens Bioelectron 2004;19:607–13. doi:10.1016/S0956-5663(03)00272-0.

[10] Lei Y, Chen W, Mulchandani A. Microbial biosensors 2006;568:200–10. doi:10.1016/j.aca.2005.11.065.

[11] Chouler J, Di Lorenzo M. Water Quality Monitoring in Developing Countries; Can Microbial Fuel Cells be the Answer? Biosensors 2015;5:450–70. doi:10.3390/bios5030450.

[12] Chouler J, Cruz-Izquierdo A, Rengaraj S, Scott J, Di Lorenzo M. A screen-printed paper microbial fuel cell biosensor for detection of toxic compounds in water. Biosens Bioelectron, 2018;102:49 - 56. doi: 10.1016/j.bios.2017.11.018.

[13] Jiang Y, Yang X, Liang P, Liu P, Huang X. Microbial fuel cell sensors for water quality early warning systems: Fundamentals, signal resolution, optimization and future challenges. Renew Sustain Energy Rev 2018;81:292-305. doi:10.1016/j.rser.2017.06.099.

[14] Wang X, Gao N, Zhou Q. Concentration responses of toxicity sensor with Shewanella oneidensis MR-1 growing in bioelectrochemical systems. Biosens Bioelectron 2013;43:264–7. doi:10.1016/j.bios.2012.12.029.

[15] Yang W, Wei X, Fraiwan A, Coogan CG, Lee H, Choi S. Fast and sensitive water quality assessment: A µl-scale

microbial fuel cell-based biosensor integrated with an air-bubble trap and electrochemical sensing functionality. Sensors Actuators, B Chem 2016;226:191–5. doi:10.1016/j.snb.2015.12.002.

[16] Stein NE, Hamelers HVM, Buisman CNJ. Stabilizing the baseline current of a microbial fuel cell-based biosensor through overpotential control under non-toxic conditions. Bioelectrochemistry 2010;78:87–91. doi:10.1016/j.bioelechem.2009.09.009.

[17] Stein NE, Hamelers HVM, Buisman CNJ. Influence of membrane type, current and potential on the response to chemical toxicants of a microbial fuel cell based biosensor. Sensors Actuators, B Chem 2012;163:1–7. doi:10.1016/j.snb.2011.10.060.

[18] Dávila D, Esquivel JP, Sabaté N, Mas J. Silicon-based microfabricated microbial fuel cell toxicity sensor. Biosens Bioelectron 2011;26:2426–30. doi:10.1016/j.bios.2010.10.025.

[19] Li F, Zheng Z, Yang B, Zhang X, Z, Lei L. A laminar-flow based microfluidic microbial three-electrode cell for biosensing. Electrochim Acta 2016;199:45–50. doi.org/10.1016/j.electacta.2016.03.138

[20] Stein NE, Hamelers HVM, Buisman CNJ. The effect of different control mechanisms on the sensitivity and recovery time of a microbial fuel cell based biosensor. Sensors Actuators, B Chem 2012;171–172:816–21. doi:10.1016/j.snb.2012.05.076.

[21] Di Lorenzo M, Thomson AR, Schneider K, Cameron PJ, Ieropoulos I. A small-scale air-cathode microbial fuel cell for on-line monitoring of water quality. Biosens Bioelectron 2014;62:182–8. doi:10.1016/j.bios.2014.06.050.

[22] Jiang Y, Liang P, Zhang C, Bian Y, Yang X, Huang X, et al. Enhancing the response of microbial fuel cell based toxicity sensors to Cu(II) with the applying of flow-through electrodes and controlled anode potentials. Bioresour Technol 2015;190:367–72. doi:10.1016/j.biortech.2015.04.127.

[23] Jiang Y, Liang P, Liu P, Miao B, Bian Y, Zhang H, Huang X. Enhancement of the sensitivity of a microbial fuel cell sensor by transient-state operation. Environ Sci Water Res Technol 2017;3:472–9. doi:10.1039/C6EW00346J.

[24] Jadhav GS, Ghangrekar MM. Performance of microbial fuel cell subjected to variation in pH, temperature, external load and substrate concentration. Bioresour Technol 2009;100:717–23. doi:10.1016/j.biortech.2008.07.041.

[25] Min B, Román ÓB, Angelidaki I. Importance of temperature and anodic medium composition on microbial fuel cell (MFC) performance. Biotechnol Lett 2008;30:1213–8. doi:10.1007/s10529-008-9687-4.

[26] Liu H, Cheng S, Logan BE. Power Generation in Fed-Batch Microbial Fuel Cells as a Function of Ionic Strength, Temperature, and Reactor Configuration. Environ Sci Technol 2005;39:5488–93. doi:10.1021/es050316c.

[27] Margaria V, Tommasi T, Pentassuglia S, Agostino V, Sacco A, Armato C, et al. Effects of pH variations on anodic marine consortia in a dual chamber microbial fuel cell. Int J Hydrogen Energy 2017;42:1820-29. doi:10.1016/j.ijhydene.2016.07.250.

[28] Agostino V, Ahmed D, Sacco A, Margaria V, Armato C, Quaglio M. Electrochemical analysis of microbial fuel cells based on enriched biofilm communities from freshwater sediment. Electrochim Acta 2017;237:133-143. doi:10.1016/j.electacta.2017.03.186.

[29] Massaglia G, Gerosa M, Agostino V, Cingolani A, Sacco A, Saracco G, Margaria V, Quaglio M. Fluid Dynamic Modeling for Microbial Fuel Cell Based Biosensor Optimization. Fuel Cells 2017;17:627–634. doi: 10.1002/fuce.201700026.

[30] Cheng S, Liu H, Logan BE. Increased performance of single-chamber microbial fuel cells using an improved cathode structure. Electrochem Commun 2006;8:489-494. doi:10.1016/j.elecom.2006.01.010

[31] Hong Y, Call DF, Werner CM, Logan BE. Adaptation to high current using low external resistances eliminates power overshoot in microbial fuel cells. Biosens Bioelectron 2011;28:71–6. doi:10.1016/j.bios.2011.06.045.

[32] Zhang G, Zhao Q, Jiao Y, Zhang J, Jiang J, Ren N, et al. Improved performance of microbial fuel cell using combination biocathode of graphite fiber brush and graphite granules. J Power Sources 2011;196:6036–41.

doi:10.1016/j.jpowsour.2011.03.096.

[33] Katuri K, Scott K, Head I, Picioreanu C, Curtis T. Microbial fuel cells meet with external resistance. Bioresour Technol 2011;102:2758-66. doi: 10.1016/j.biortech.2010.10.147.

[34] Akhtar F, Rehmani MH. Energy replenishment using renewable and traditional energy resources for sustainable wireless sensor networks: A review. Renew Sustain Energy Rev 2015;45:769-784. doi:10.1016/j.rser.2015.02.021.

[35] Russell AD, Hopwood D. The Biological Uses and Importance of Glutaraldehyde. Progress in Medicinal Chemistry 1976; 13:271-301. doi.org/10.1016/S0079-6468(08)70140-1.

[36] Leung HW. Aerobic and anaerobic metabolism of glutaraldehyde in a river water-sediment system. Arch Environ Contam Toxicol 2001;41:267-73. doi:10.1007/s002440010248.

[37] McGucken PV, Woodside W. Studies on the Mode of Action of Glutaraldehyde on Escherichia coli. J Appl Bacteriol 1973;36:419–426. doi:10.1111/j.1365-2672.1973.tb04123.x.

[38] Macomber L, Hausinger RP. Mechanisms of nickel toxicity in microorganisms. Metallomics 2011;3:1153–62. doi:10.1039/c1mt00063b.

[39] Xu Z, Liu B, Dong Q, Lei Y, Li Y, Ren J, et al. Flat microliter membrane-based microbial fuel cell as “on-line sticker sensor” for self-supported in situ monitoring of wastewater shocks. Bioresour Technol 2015;197:244-251. doi:10.1016/j.biortech.2015.08.081.

[40] Cervantes C, Campos-Garcı´a J, Devars S, et al. Interactions of chromium with microorganisms and plants. FEMS Microbiology Reviews 2001;25:335–347. doi.org/10.1016/S0168-6445(01)00057-2.

[41] Tchounwou PB, Yedjou CG, Patlolla AK, Sutton DJ. Heavy Metal Toxicity and the Environment. In: Luch A. (eds) Molecular, Clinical and Environmental Toxicology. Experientia Supplementum 2012; 101. Springer, Basel. doi:10.1007/978-3-7643-8340-4_6.

[42] Lamb A, Tollefson EL. Toxic effects of cupric, chromate and chromic ions on biological oxidation. Water Res 1973;7:599-613. doi.org/10.1016/0043-1354(73)90060-2.

[43] Saida S, Abdelkader G. Inhibition of chrome (III) on the activated sludge activity. Environ Technol 1994; 15:255-262. doi.org/10.1080/09593339409385426.

[44] Tommasi T, Salvador GP, Quaglio M. New insights in Microbial Fuel Cells: novel solid phase anolyte. Scientific Reports, 2016;6: 29091.

[45] Massaglia G, Margaria V, Sacco A, Tommasi T, Pentassuglia S, et al. In situ continuous current production from marine floating microbial fuel cells. Applied Energy 2018;230:78-85.

[46] Olatinwo SO, Joubert T-H. Optimizing the Energy and Throughput of a Water-Quality Monitoring System. Sensors (Basel), 2018;18:1198

FIGURE AND TABLE LEGENDS

Figure 1. Overview of the structure of the experimental phases of the MFCs. As presented in Figure 7, each toxic cycle was followed by recovery cycles with non-toxic medium.

Figure 2. Performance of MFCs under 47Ω and 1kΩ external load compared to the room temperature variation profile.

Figure 3. Non-toxic response of MFC biosensors in semi-continuous operation mode. Current density profile of 2 non-toxic cycles for the two MFCs employed is shown. The red dashed lines indicate the end of feeding period. The influent is composed by a fixed acetate concentration of 1 g L-1 and a constant pH value of 7 (phosphate buffer).

Figure 4. MFC biosensor responses to glutaraldehyde (5-1000 ppm). A) Current density output versus time. The reported current densities are relative to a single representative MFC (duplicate reported in supplementary information Figure S3). The vertical dashed line indicates the end of feeding period. B) Linear fit of the current change after 4 h (the difference between the current density produced as a response to toxicant feeding and that of control (non-toxic feeding)) of feeding versus glutaraldehyde concentration. Each data point is the average from the two MFCs. The error bars represent the standard deviation. C) Inhibition ratio calculated using eq. **a** and **b**. The values are the average of the two MFCs ± standard deviation.

Figure 5. MFC biosensors response towards nickel(II). A) Nickel(II) toxic tests: current density output versus time. The reported current densities are relative to a single representative MFC (duplicate reported in supplementary Figure S3). The vertical dashed line indicates the end of feeding period; B) Linear fit of the current change after 4 hours (i.e. the variation in current density values at the exact time point) of feeding versus Ni^{2+} concentration. Each point is the average of data obtained from the two MFCs. The error bars represent the standard deviation. C) Inhibition ratio calculated using eq. **a** and **b**. The values are the average of the two MFCs ± standard deviation.

Figure 6. Response of MFC biosensors to chromium(III). A) Current density output versus time. The reported current densities are relative to a single representative MFC (duplicate reported in supplementary information Figure S3). The vertical dashed line indicates the end of feeding period. B) Inhibition ratio calculated using eq. **a** and **b**. The values are the average of the two MFCs ± standard deviation.

Figure 7. Current density profile of one MFC during toxicant detection experiment, from days 1 to 30. To depict an exhaustive overview of the experiment only the highest concentration of toxicants and their subsequent recovery cycles are shown. No recovery was performed after 20 mg L^{-1} of Cr^{3+}.

Figure 8. Current density profile of a non-toxic feeding cycle before glutaraldehyde toxicity test (black dotted curve) and its first derivative as a function of time (blue curve). The maxima and minima of the first derivative correspond to the 3 critical time points used to highlight anomalies and toxicants presence in the MFC influent.

Table 1. Comparison of the steady-state non-toxic feeding cycles before each different toxicant experiment, in terms of current density values after 4 hours of feeding and total coulombic yield, and the resulting degree of recovery. The values represent the average of the two MFCs ± standard deviation.

Table 1 Comparison of the steady-state non-toxic feeding cycles before each different toxicant experiment, in term of total coulombic yield and current density values after 4 hours of feeding, and the resulting degree of recovery. The values represent the average of the two MFCs ± standard deviation.

Cycles	Total Coulombic Yield (C)	Degree of recovery (%)	Current density after 4 hs of feeding (mA m^{-2})	Degree of recovery (%)
Non-toxic before Glut.	19.1 ± 1.6	-	391 ± 14	-
Non-toxic before Ni^{2+}	22.2 ± 1.5	116	410 ± 11	105
Non-toxic before Cr^{3}	16.9 ± 0.9	88.5	378 ± 13	97

Table 2. Inhibition ratios based on current density value at the 3 critical times points (ctp). Early toxicity corresponds to ctp1; mid-term toxicity corresponds to ctp2 and late toxicity corresponds to ctp3. The total toxicity consists of the sum of the three inhibition values. The values reported are the average of the two MFCs ± standard deviation.

Table 2 Inhibition ratios based on current density value at the 3 critical times points. Early toxicity corresponds to ctp1; mid-term toxicity corresponds to ctp2 and late toxicity corresponds to ctp3. The total toxicity consists of the sum of the inhibition values. The values reported are the average of the two MFCs ± standard deviation.

Glutaraldheyde	I_{ctp1} (%) Early-toxicity	I_{ctp2} (%) Mid-term toxicity	I_{ctp3} (%) Late toxicity	I_{tot} Overall toxicity
5 ppm	10.6 (±3.2)	6.1 (±1.9)	-9.2 (±1.0)	7.4 (±1.7
50 ppm	12.8 (±3.9)	8.9 (±1.4)	-11.7 (±1.5)	10.0 (±0.6)
500 ppm	13.8 (±1.2)	17.1 (±1.0)	26.2 (±1.1)	57.1 (±0.2)
1000 ppm	36.8 (±0.7)	33.3 (±2.1)	58.1 (±2.8)	128.2 (±0.9)
Nickel (II)	I_{ctp1} (%) Early-toxicity	I_{ctp2} (%) Mid-term toxicity	I_{ctp3} (%) Late toxicity	I_{tot} (%) Overall toxicity

2 mg L^{-1}	0.0 (±1.0)	0.0 (±1.0)	0.0 (±1.0)	0.0 (±1.0)
20 mg L^{-1}	-3.0 (±0.9)	5.2 (± 0.8)	11.2 (±1.2)	13.4 (±0.7)
60 mg L^{-1}	19 (±2.0)	9.1(± 1.1)	27.3 (±0.9)	55.4 (±0.9)

Chromium (III)	**I_{ctp1} (%)** **Early-toxicity**	**I_{ctp2} (%)** **Mid-term toxicity**	**I_{ctp3} (%)** **Late toxicity**	**I_{tot} (%)** **Overall toxicity**
2 mg L^{-1}	0.0 (±1.0)	0.0 (±1.0)	0.0 (±1.0)	0.0 (±1.0)
20 mg L^{-1}	1.8 (±0.5)	3.2 (± 0.1)	32.3 (±0.9)	37.3 (±0.9)

Non controlled T° conditions; pH 7; fixed [acetate] of 1 g L^{-1}

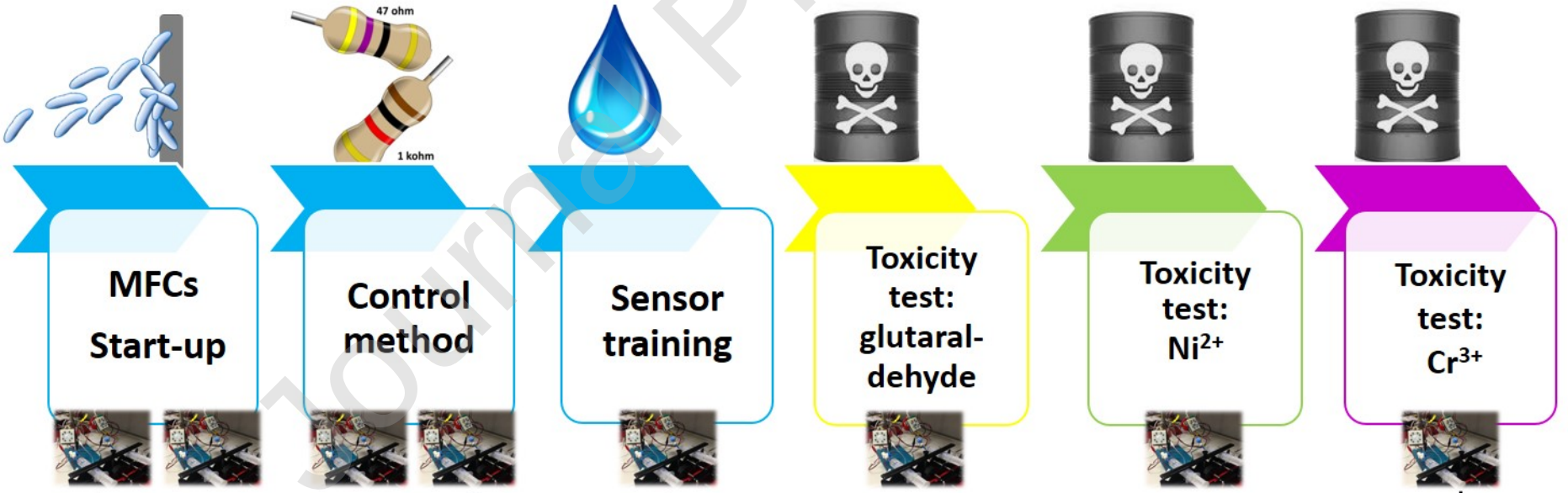

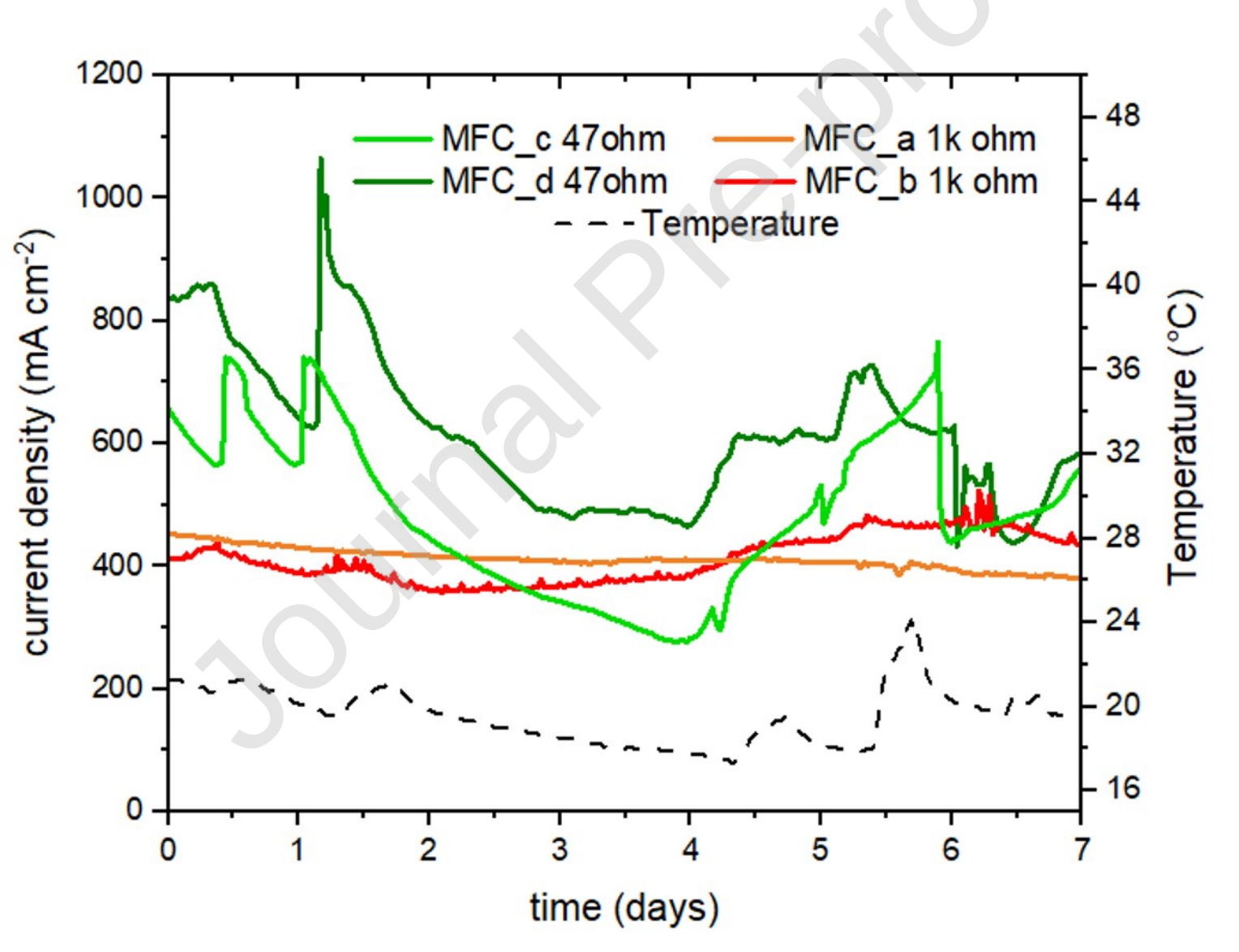

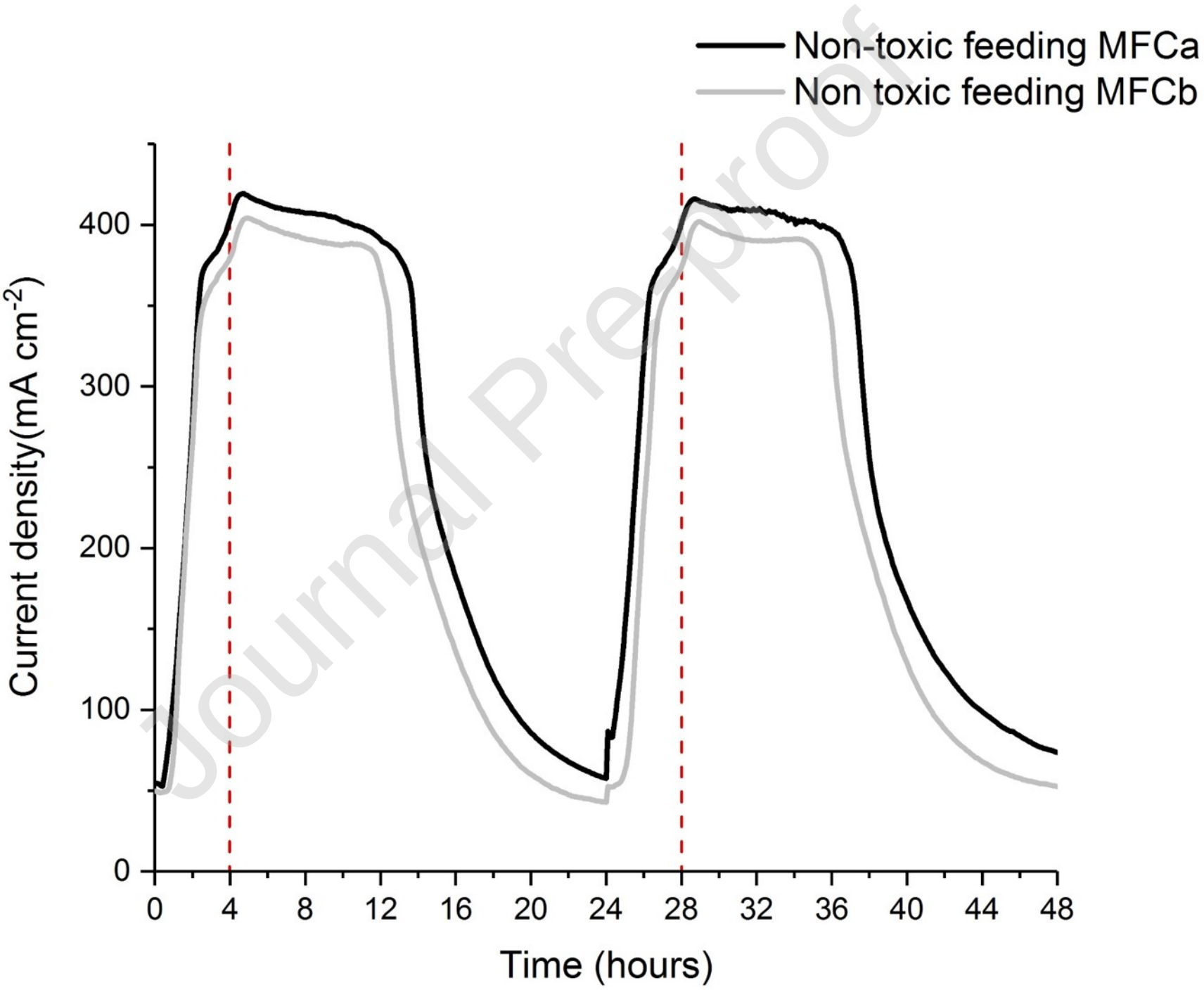

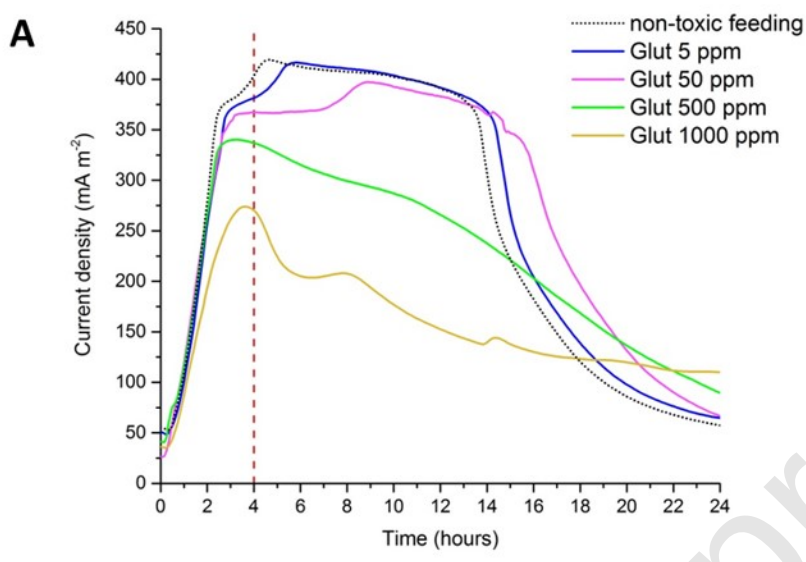

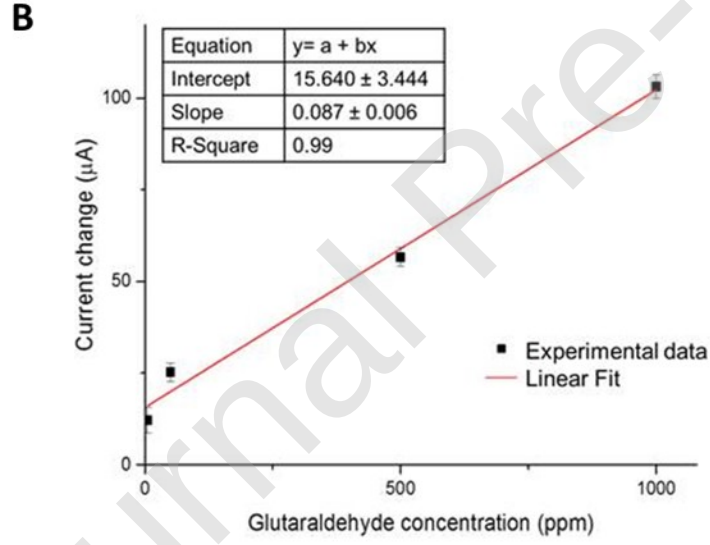

C

Glutaraldheyde Concentration (ppm)	Inhibition ratio % based on j after 4 hs / I_{4hs}	Inhibition ratio % based on tot. coulombic yield / I_C
5	3.4 (±1.0)	-0.9 (±2.0)
50	7.1 (±1.9)	-5 (±1.3)
500	16.1 (±0.4)	13.4 (±1.5)
1000	29.2 (±3.8)	39.9 (±1.2)

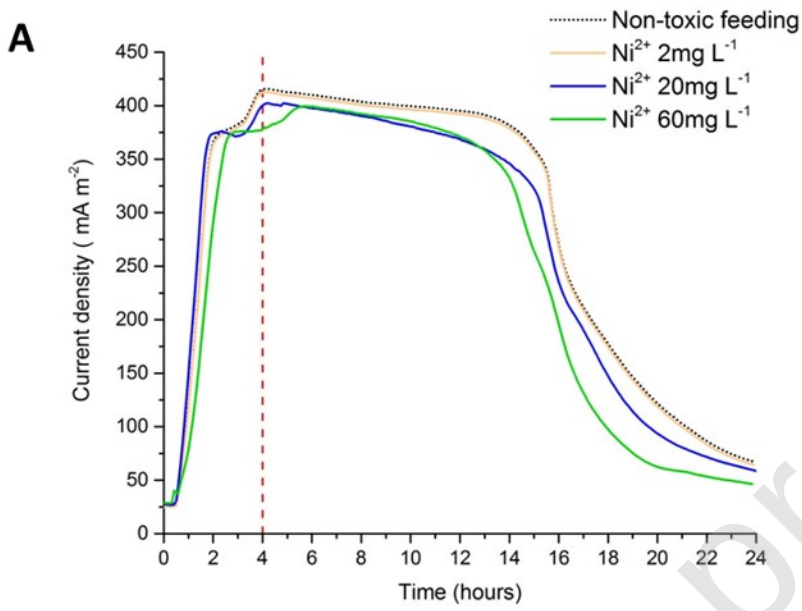

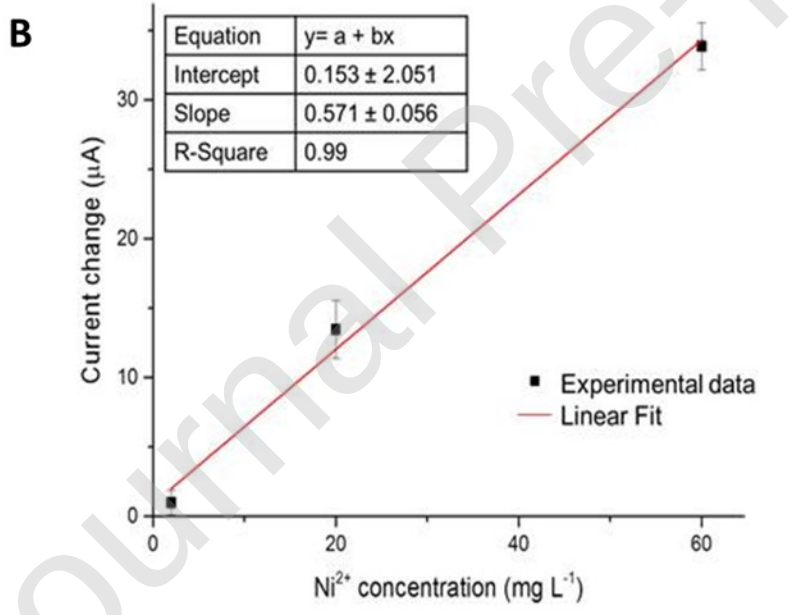

C

Nickel (II) mg L^{-1}	Inhibition ratio % based on j after 4 hs / I_{4hs}	Inhibition ratio % based on tot. coulombic yield / I_C
2	0.0 (±1.1)	0.0 (±1.5)
20	4.8 (±1.8)	6.2 (±0.8)
60	9.2 (±2.9)	13.4 (±2.1)

A

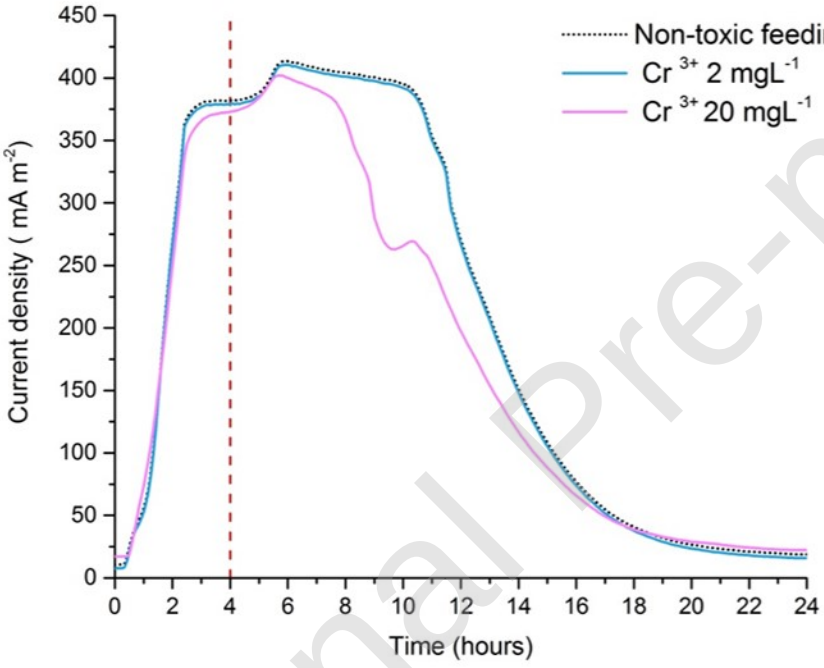

B

Chromium (III) mg L^{-1}	Inhibition ratio % based on j after 4 hs / I_{4hs}	Inhibition ratio % based on tot. coulombic yield / I_C
2	0.0 (±0.6)	0.0 (±0.4)
20	2.4 (±0.4)	13.3 (±1.3)

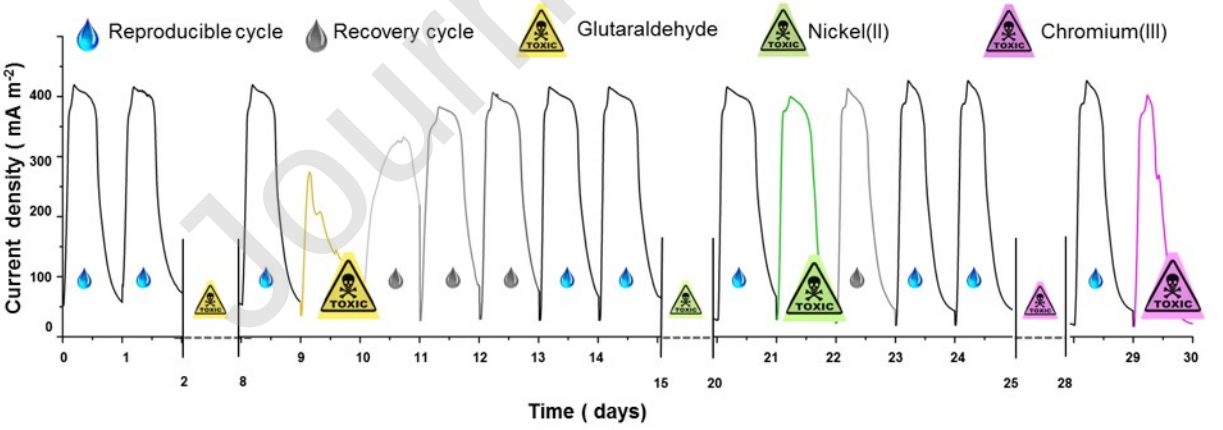
Reproducible cycle
Recovery cycle
Glutaraldehyde
Nickel(II)
Chromium(III)
TOXIC
Current density (mA m-2)
0
100
200
300
400
0
1
2
8
9
10
11
12
13
14
15
20
21
22
23
24
25
28
29
30
Time (days)

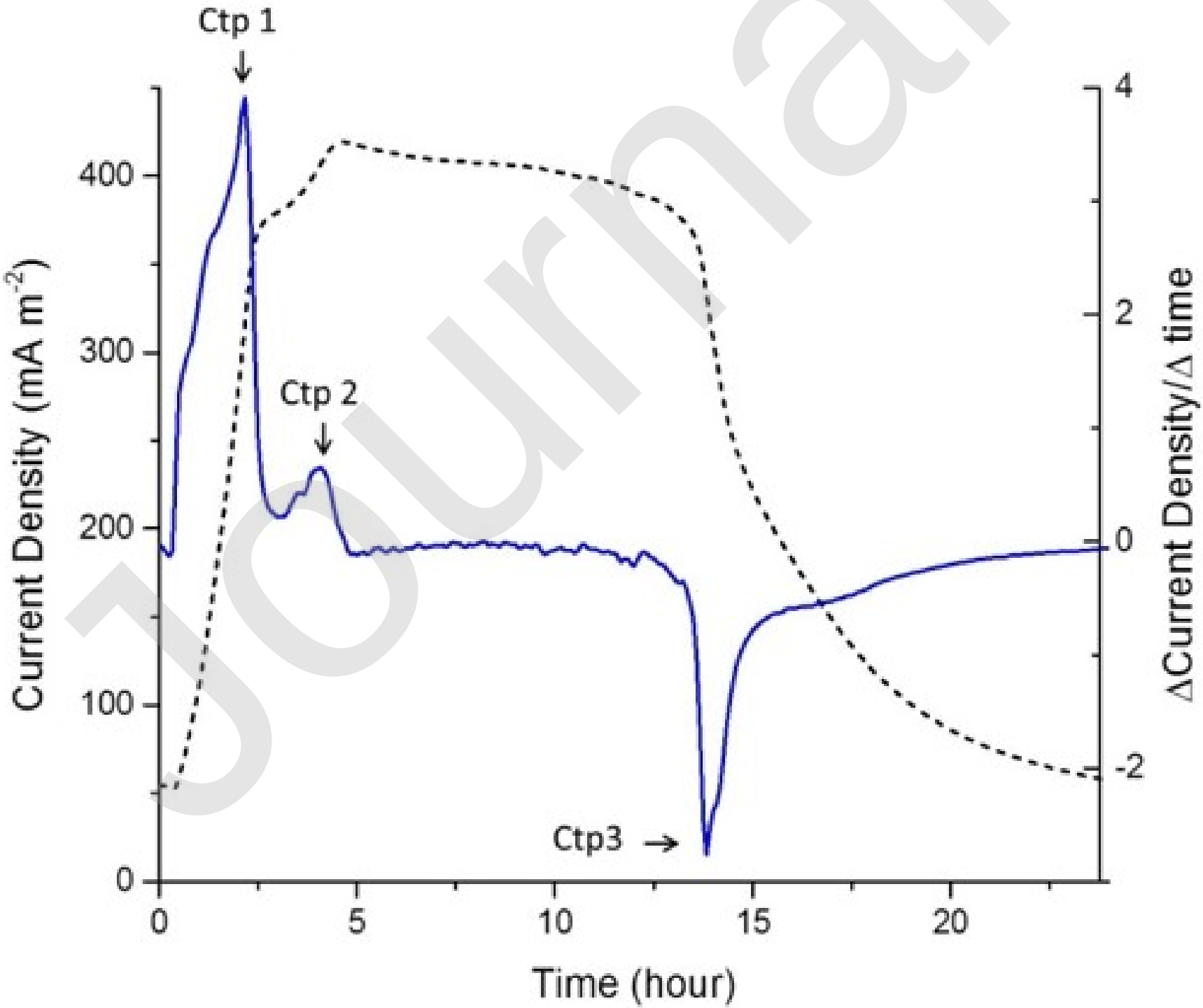
Ctp 1
Ctp 2
Ctp3
Current Density (mA m-2)
ΔCurrent Density/Δ time
Time (hour)
0
100
200
300
400
0
5
10
15
20
4
2
0
-2